

Cite this: *Chem. Sci.*, 2025, 16, 2710

All publication charges for this article have been paid for by the Royal Society of Chemistry

B(MIDA)-directed site-selective intermolecular halofluoroalkylation of alkenes: synthesis of diversely functionalized building blocks†

Hengbo Wu,^{‡ab} Ruitong Luo,^{‡ab} Jingjing Peng,^{ab} Zijian Han,^{ab} Renjie Zhang,^{bc} Zhijian Xu,^{ibab} Weiliang Zhu,^{ibab} Hong Liu^{ibab}* and Chunpu Li^{ibab}*

α -Halo borides are generally constructed via Matteson homologation, and the synthesis of both fluorinated and functionalized ambiphilic boronates is challenging and has received inadequate attention. Herein, we describe the *N*-methyliminodiacetyl boronate [B(MIDA)]-directed halogenation of alkenes via a complementary sequence involving fluoroalkyl radical addition followed by guided radical-to-metal oxidative addition and C–X reductive elimination. The alkali cation and functional groups in B(MIDA) enable coulombic interaction and weak attraction with halogens, which could weaken the Pd–X bond and assist in C–X bond formation and is verified by DFT calculations. As a result, a wide variety of highly functionalized fluorinated α -halo boronates, including drugs and natural products, are obtained in good or moderate yields through the unique catalytic manifold. Notably, the trifunctionalized (F, X, B) building block could be transformed into diverse modified fluorinated products.

Received 22nd November 2024

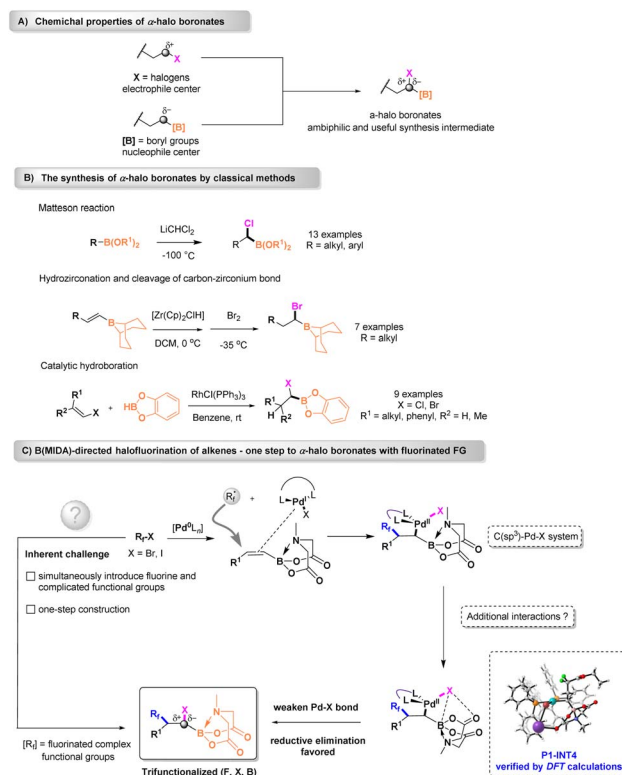
Accepted 29th December 2024

DOI: 10.1039/d4sc07900k

rsc.li/chemical-science

Introduction

The α -halo alkylboronic esters containing two reacting functional groups are invaluable synthons for the construction of C–O, C–N, and C–C bonds, which makes them useful for organic synthesis and the total synthesis of natural products.^{1–5} The α -halo borides, indeed, serve as ambiphilic reagents with both electrophile (C–X) and nucleophile (C–B) centers (Scheme 1A). As an appealing synthesis intermediate, applications in cross-couplings to secondary alkylboronate esters under mild nickel-catalyzed conditions have been disclosed recently.^{6–8} Moreover, transformations from halogens into amines enable the construction of valuable α -amino boronates, which play a pivotal role in the total synthesis of FDA-approved drugs such as Bortezomib.⁹ Numerous studies have attempted to exploit effective reactions for the synthesis of α -halo borides (Scheme 1B). Generally, ambiphilic boron reagents are prepared through Matteson homologation,¹⁰ a process involving concerted 1,2-



Scheme 1 Reaction design.

^aState Key Laboratory of Drug Research, Shanghai Institute of Materia Medica, Chinese Academy of Sciences, Shanghai 201203, China. E-mail: wlzhu@simm.ac.cn; hliu@simm.ac.cn; lichunpu@simm.ac.cn

^bUniversity of Chinese Academy of Sciences, No.19A Yuquan Road, Beijing 100049, China

^cSchool of Pharmaceutical Science and Technology, Hangzhou Institute for Advanced Study, University of Chinese Academy of Sciences, Hangzhou, 310024, China

† Electronic supplementary information (ESI) available: Full experimental details, characterization data, and original ¹H and ¹³C NMR spectra. CCDC 2236620 (for 23). For ESI and crystallographic data in CIF or other electronic format see DOI: <https://doi.org/10.1039/d4sc07900k>

‡ These authors contributed equally to this work.

metallate rearrangement. However, applying this protocol to the formation of specific boronates is challenging owing to the extremely low temperature and harsh preparation conditions of the organometallic reagent (LiCHCl_2). Additionally, in most cases prefunctionalized primary borides, in which simple substitution groups such as linear alkyl, phenyl, and seldom polar units are limited, could be utilized. As a supplement, catalytic hydroboration,¹¹ catalytic hydrohalogenation,¹² and photo-induced methodologies¹³ are alternative approaches, but the substrate scope is limited. The need for moisture or air-sensitive reagents and complicated operations limits the widespread synthetic applications of the abovementioned approaches. Lately, Wang¹⁴ and Xu¹⁵ reported two elegant strategies involving the radical C–H halogenation of benzyl borides and deoxygenative haloboration from carbonyls. Although some intriguing examples have recently been described, the synthesis of α -halo borides is expected to be very challenging, because these substrates tend to undergo dehalogenation or β -hydride elimination. In addition to some complex functional groups, the concurrent one-step incorporation of fluorine, which has been emphasized in several fields including the pharmaceutical, agrochemical, and material industries,^{16–18} remains a daunting task. To the best of our knowledge, only a handful of fluorinated iodides, most of which are perfluoroalkyl iodides, could be utilized to form the particular product.¹⁹ Thus, developing efficient and facile synthetic patterns for forging diverse fluorine-containing α -halo borides is in high demand.

We anticipated that a site-oriented α -halogenation could be achieved using the borides. Pioneered by Burke and co-workers, *N*-methyliminodiacetyl boronates [B(MIDA)s] have been identified as a purifiable, stable, and compatible surrogate for traditional boronates²⁰ and the use of B(MIDA)s has been helpful in overcoming various obstacles in synthesizing challenging organoboron compounds.^{21–23} Conceptually, inspired by a *N*-tetranuclear organoboron catalyst which was similar to the B–N-containing BMIDA group,^{24–26} we envisioned that potential interactions between boron/nitrogen/oxygen in BMIDA and halogen atoms might be helpful for orienting halogens. Fluoroalkyl halides (R_fX), an ideal functionalized fluorine source, could be initiated by palladium to generate fluoroalkyl radicals.^{27,28} Building on the above principles, we employed olefin B(MIDA) derivatives that could undergo a free fluorine radical recombination after the Pd(0) activation, to generate the key Pd(I)–X species and reactive α -borylalkyl radicals.^{29,30} Consequently, colligation of the mentioned species would result in a $\text{C}(\text{sp}^3)\text{--Pd}(\text{II})\text{--X}$ system where direct reductive elimination is thermodynamically disfavored.³¹ Computational studies have proved that X–Pd(II) dissociation was a critical step in the $\text{C}(\text{sp}^3)\text{--Pd}(\text{II})\text{--X}$ RE process,³² so we supposed that additional interactions resulting from functional groups in BMIDA could reduce the Pd-center electron density and therefore facilitate heterolytic bond dissociation. Presumably, the potential X–B attraction and alkali metal cation aided³³ coulombic interaction were thought to suppress the kinetic hindrance and then lead to direct reductive elimination. Finally, α -halo boronates characterized by useful trifunctionalized building blocks may serve as

a platform for further decorations (Scheme 1C). Herein, we report the B(MIDA)-dictated palladium-catalyzed halo-fluoroalkylation of alkenes with fluoroalkyl halides (R_fX) and the detailed mechanism was revealed by density functional theory (DFT) calculations. In contrast to the existing methods that rely on sophisticated manipulations to prepare starting organoboron precursors, this unique technique is characterized by high efficiency, synthesis simplicity, the commercial availability of reagents, and a remarkably broad substrate scope, thus allowing for straightforward access to fluorinated α -halo boronates even for the late-stage modification of biologically relevant systems, which may be widely applied to medicinal chemistry and chemical biology.

Results and discussion

Considering the significant role of difluoromethylene (CF_2) in improving the physicochemical and biological properties of drugs and natural products,³⁴ we conducted our investigation using the commercially available bromodifluoroacetate, which has been intensively developed,³⁵ and vinyl B(MIDA) for the construction of fluorinated α -halo boronates (Table 1).

To test our hypothesis, a variety of palladium catalysts, ligands, bases, and solvents were applied for the model reaction. Remarkably, a combination of $\text{PdCl}_2(\text{dppf})\cdot\text{DCM}$ (10 mol%) with an electron-rich racemic BINAP ligand in the presence of a Brønsted base K_2CO_3 in ethyl acetate at 85 °C could generate the desired product in a 90% yield, as determined *via* ^{19}F NMR (entry 1, for detailed optimization studies, see Tables S1–S4, ESI†). Even the standard condition was similar to that employed in Heck coupling, no Heck-type product was detected and **1** was formed in a moderate yield (entry 2) regardless of the presence of an argon atmosphere. Among the palladium catalysts, $\text{PdCl}_2(\text{dppf})\cdot\text{DCM}$ exerted the

Table 1 Optimization of the reaction conditions^a

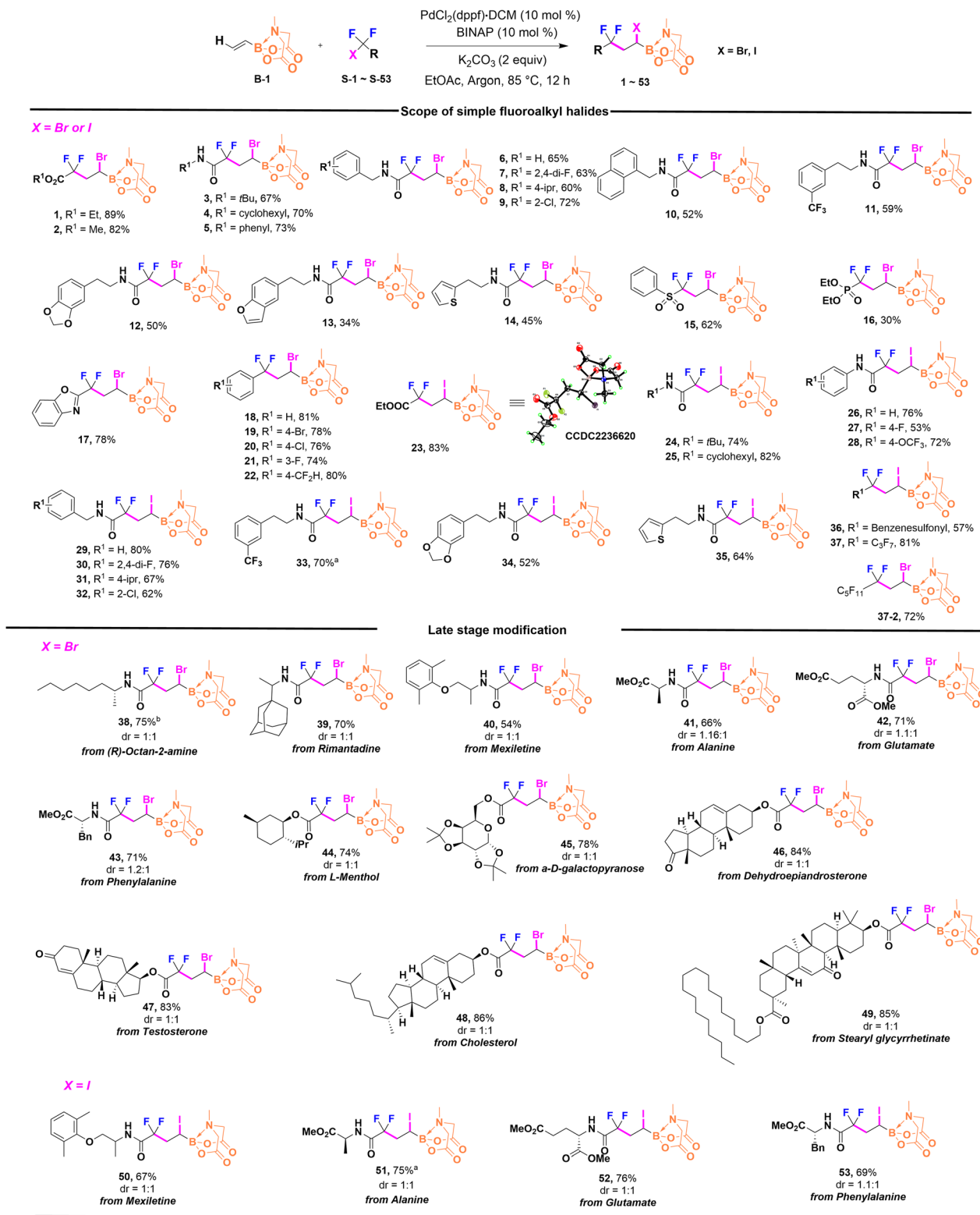
Entry	Deviation from standard conditions	Yield ^b
1	None	90 (89)
2	Air	66
3	$\text{PdCl}_2(\text{MeCN})_2$ instead of $\text{PdCl}_2(\text{dppf})\cdot\text{DCM}$	59
4	Dppe instead of BINAP	15
5	^t BuOK instead of K_2CO_3	23
6	Dioxane instead of EtOAc	61
7	S-1 (4 equiv.)	70
8	Without K_2CO_3	<5

^a Reaction conditions: **B-1** (0.27 mmol, 1.0 equiv.), **S-1** (2.0 equiv.), $\text{PdCl}_2(\text{dppf})\cdot\text{DCM}$ (10 mol%), BINAP (10 mol%), K_2CO_3 (2.0 equiv.), EtOAc (2 mL), 85 °C, argon, 12 h, if otherwise noted. ^b Determined by ^{19}F NMR using fluorobenzene as an internal standard, and the number in parentheses is the isolated yield.



best catalytic activity, which surpassed that of $\text{PdCl}_2(\text{MeCN})_2$ (entry 3). Specifically, variation from BINAP to Dppe resulted in a decreased yield (15%), which suggests that maintaining the steric hindrance of the ligand was essential for the reaction

(entry 4). Moreover, a relatively low yield was achieved *via* $t\text{BuOK}$ utilization (entry 5). Replacing ethyl acetate with dioxane still provided **1** in a moderate yield, indicating that the reaction was relatively insensitive to the change of solvent (entry 6). Likewise,



Scheme 2 Substrate scope of fluorides. Reaction conditions: B(MIDA) (0.27 mmol, 1.0 equiv.), fluorides (2.0 equiv.), $\text{PdCl}_2(\text{dppf})\cdot\text{DCM}$ (10 mol%), BINAP (10 mol%), K_2CO_3 (2.0 equiv.), EtOAc (2 mL), 85 °C, argon, 12 h. ^aThe reaction was conducted in air. ^bThe reaction was conducted for 5 h.



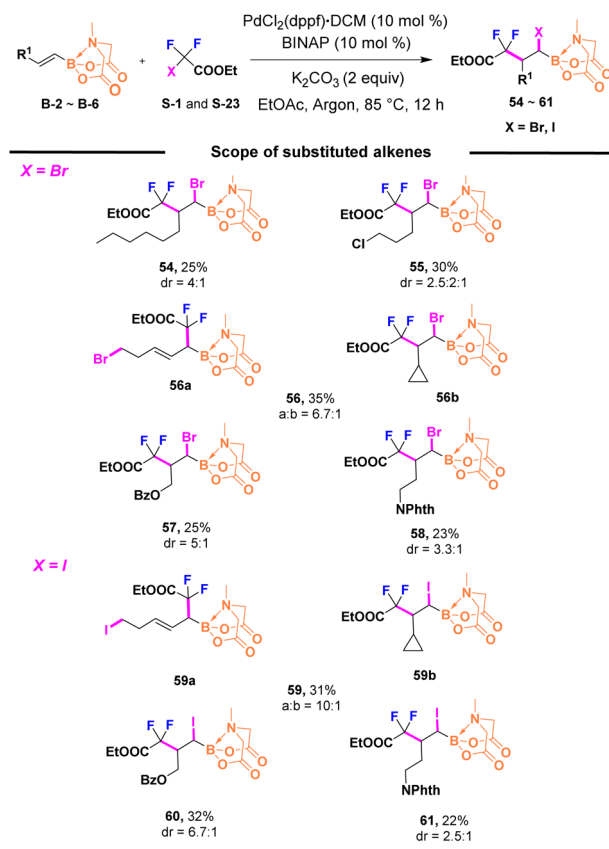
a good yield of **1** was achieved at a high **S-1** amount of 4 equiv. (entry 7). The lack of K_2CO_3 significantly reduced the reaction yield (entry 8).

To gain some insights into the reaction's compatibility with different functional groups, under the optimized reaction conditions, we first explored the scope of bromodifluoro esters and amides. Accordingly, the methyl ester derivate (**2**) was well applicable to the reaction, with a yield of 82%. As demonstrated in Scheme 2, the protocol was found to be general and characterized by remarkable tolerance in the presence of amides with commonly encountered fragments. The steric hindrance of amines with *tert*-butyl (**3**) and cyclohexyl (**4**) could provide the corresponding products, with yields of ~70%. Aniline and benzylamine derivatives containing electron-withdrawing difluoro, chlorine, and trifluoromethyl were smoothly processed (**5-7**, **9**, **11**), which provides good opportunities for downstream transformations. The benzylamines containing isopropyl (**8**) and naphthalene (**10**) underwent a successful reaction, although the yields were moderate. Versatile synthetic handles, such as electron-donating methylenedioxy, heterocyclic benzofuran, and thiophene were all compatible under the standard conditions (**12-14**). Encouraged by the above-mentioned results, we sought to examine other bromodifluoro sources including phenyl sulfone, diethyl phosphonate, and benzo[d]oxazole, and the direct substitution of benzene (**15-22**). In the cases of sulfone (**15**) and phosphonate (**16**), the reaction was less efficient than the reactions involving the above substrates. Nevertheless, the oxazole ring (**17**) and other aryl halides (**18-22**) exhibited promising tolerance, attributable to reactive benzyl radicals generated by palladium catalysts. In addition to the universality of bromo, we questioned whether this strategy could enable the creation of iodofluorinated products. Surprisingly, α -iodo B(MIDA) boronates were also readily generated using the corresponding iodofluorides. The ester (**23**), alkyl amines (**24**, **25**), and aniline (**26**) could be successfully converted into the corresponding products, with similarly high levels of yields. The structure of **23** was identified *via* X-ray crystallography. Considering the two electron-withdrawing groups, OCF_3 -substituted aniline (**28**) maintained a good yield, while the F-substituted one (**27**) showed a moderate yield. Regarding the benzylamines (**29-33**), the method was also applicable, regardless of the electrical properties, and was more efficient than the bromo products. Of note, product **33** could be conveniently achieved with no difficulties when argon was displaced by air. In terms of methylenedioxy (**34**) and thiophene (**35**), the required products were obtained with moderate efficiency. Moreover, other types of iodofluorides, for instance, phenyl sulfone (**36**), were applicable under standard conditions, and particularly, perfluoroalkyl iodide (**37**) and perfluoroalkyl bromide (**37-2**) were installed at the right position, with excellent yields, owing to the convenient initiation from palladium catalysts.^{27c,28}

Then, we modified the bioactive molecules with complex motifs. To our delight, a chiral-derived compound **38** was generated in a 75% yield. For the decorations of drugs, mexiletine, a drug against ventricular arrhythmia, and rimantadine, a drug with great influence on the influenza virus, were

modified to provide **39** in a 70% yield and **40** in a 54% yield. As a critical area in biology research, a series of amino acid substrates from alanine, glutamate, and phenylalanine were tested to evaluate the generality of the palladium-catalyzed system, where all products were furnished smoothly (**41-43**). Further exploration using *L*-menthol (**44**) and α -D-galactopyranose (**45**) from carbohydrates was highly efficient, as proved by the good yields. Prominently, transformations proceeded excellently in the presence of steroids (**46-48**) and pentacyclic triterpene (**49**) under standard conditions. The assembly of **46** and **48**, which possess internal alkenes, yielded predominantly addition products neighbored by boron atoms with good site-selectivity, suggesting a directing effect of the B(MIDA) moiety on the adjacent alkene. The above results demonstrated that the current method was applicable to biologically relevant systems, thereby expanding the utilization scope of the reaction for convenient late-stage modifications. Moreover, iodofluorides from mexiletine (**50**) and amino acids (**51-53**) could produce expected products, with yields of 67%, 75%, 76%, and 69%, respectively.

Next, we concluded that the reaction could be extended to even substituted olefins with B(MIDA). As illustrated in Scheme 3, the majority of substrates suffered from relatively low yields largely because of the stabilized hyperconjugation effect on the



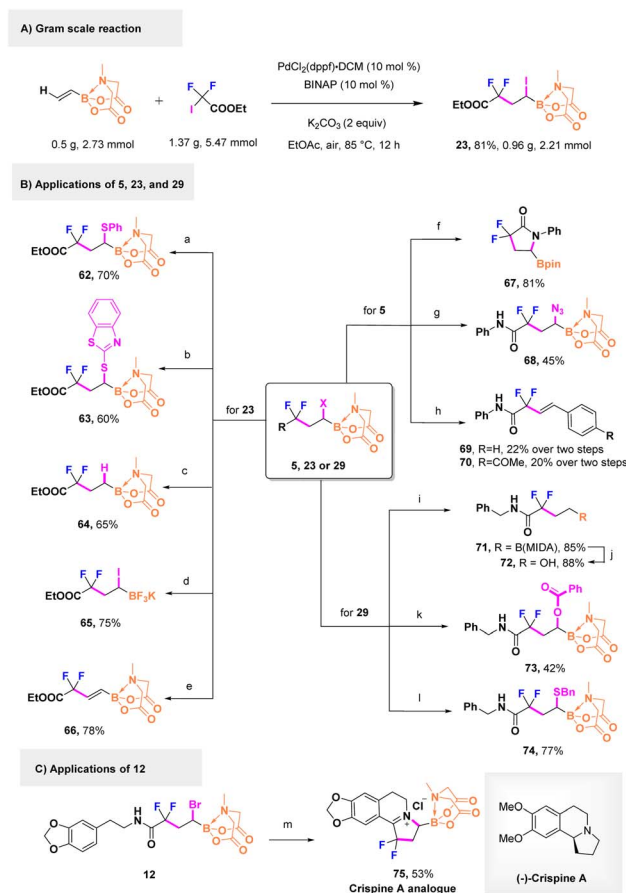
Scheme 3 Substrate scope of substituted olefin B(MIDA)s. Reaction conditions: B(MIDA) (0.27 mmol, 1.0 equiv.), fluorides (2.0 equiv.), $PdCl_2(dppf) \cdot DCM$ (10 mol%), BINAP (10 mol%), K_2CO_3 (2.0 equiv.), EtOAc (2 mL), 85 °C, argon, 12 h.



substituted radicals. Alkyls (**54**) and halogens such as chlorine (**55**) were amenable to the general method. An attractive rearrangement product (**56a**) bearing cyclopropyl as the starting material was unexpectedly generated, which broadened the vision of constructing α -difluoromethylene (CF_2)-containing B(MIDA) boronates and indirectly verified the radical process occurring in this reaction. The ratio of **56a** to **56b** was 6.7 : 1 according to the ^{19}F NMR analysis. In addition to the above compounds, functionalized side chains possessing benzoyl (**57**) and phthalimide (**58**) groups were tolerant to the established reaction. Consistent with the non-substituted examples, iodine could be installed properly when substituted olefins were employed. The rearrangement iodinated product **59a** was afforded in a 31% yield, including 10% **59b**. Benzoyl (**60**) and phthalimide (**61**) substrates could be transformed into the corresponding iodine-containing boronates, in which preliminary diastereoisomer ratio values were observed: 6.7 : 1 for **60** and 2.5 : 1 for **61**, respectively.

In view of the potential synthetic building blocks of fluorinated α -halo boronates, the advantage of this strategy has also been exemplified by the efficient gram-scale synthesis of product **23**, and 81% isolated yield was obtained under air conditions (Scheme 4A). The presence of different esters and amides provided valuable opportunities for diverse organic applications as privileged trifunctionalized moieties. As shown in Scheme 4B, starting from **23**, the iodine could be easily substituted by nucleophilic benzenethiol derivatives in good yields (**62** and **63**). This special iodine was not only selectively dehalogenated but also eliminated readily to furnish fluorinated vinyl and alkyl B(MIDA) boronates (**64** and **66**) in moderate yields. Treating **23** with KHF_2 could afford its BF_3K analog (**65**). We also examined the prospect of using bromine atoms. Treating **5** with sodium azide could yield a C–N bond containing derivative **68**. Moreover, treating **5** with pinacol under an alkaline condition could generate difluoropyrrolidine pinacol boronates (**67**) for the first time in high yield. The coupling nature of B(MIDA) boronates was leveraged during the mixing of eliminated-**5** with benzene halides to produce styrene-Heck-type compounds **69** and **70**. Furthermore, an amide group-bearing compound **29** could smoothly yield benzylmercaptan together with benzoate substituted products, which constructed C–O (**73**) and C–S (**74**) bonds directly. The dehalogenation intermediate (**71**) of **29** was oxidized, during which the B(MIDA) motif was converted into the hydroxyl group (**72**) for further transformation. Fortunately, treating **12** via a Bischler–Napieralski reaction led to the generation of an unprecedented fluorinated crispine A analog (**75**) in an acceptable yield, which offers a new approach to tetrahydroisoquinoline engineering (Scheme 4C).

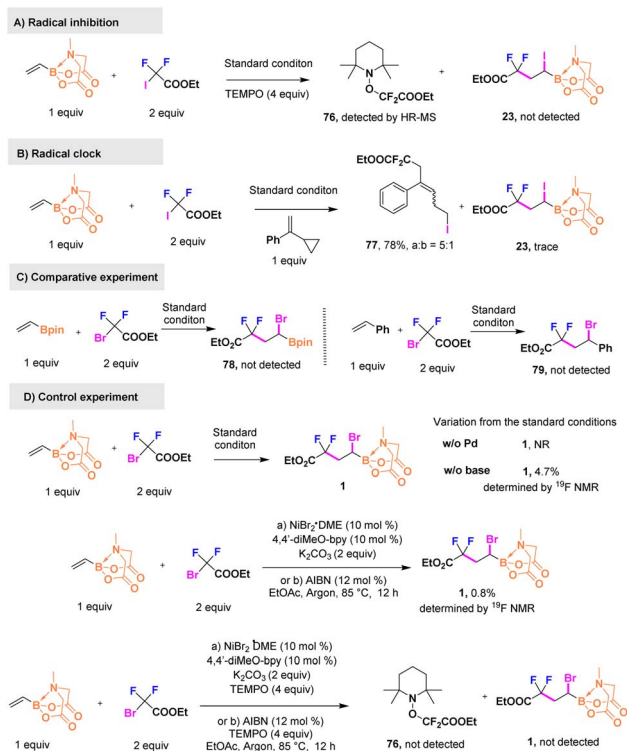
Furthermore, we investigated the mechanistic aspects of the palladium catalytic cycle and highlighted the role of the B(MIDA) moiety. To identify whether a difluoroalkyl free radical was involved in the process, a mixture of vinyl B(MIDA) and ICF_2COOEt was treated with the radical scavenger TEMPO. As depicted in Scheme 5A, no desired product was detected, and a TEMPO– CF_2COOEt complex **76** was validated *via* high-resolution mass spectrometry. A radical clock experiment was



Scheme 4 Gram-scale preparation and synthetic utilities. Reaction conditions: for the gram scale reaction: B(MIDA) (2.73 mmol, 1.0 equiv.), ICF_2COOEt (2.0 equiv.), $\text{PdCl}_2(\text{dppf})\cdot\text{DCM}$ (10 mol%), BINAP (10 mol%), K_2CO_3 (2.0 equiv.), EtOAc (10 mL), 85 °C, air, 12 h. ^aPhSNa, DMF, 85 °C; ^bsodium benzo[d]thiazole-2-thiolate, DMF, 85 °C; ^cTTMSS, PhMe, 85 °C; ^d KHF_2 , MeOH, 70 °C; ^e BnNH_2 , DMF, 85 °C; ^fpinacol, K_3PO_4 , DCM/THF/ H_2O , 60 °C; ^g NaN_3 , DMF, 85 °C; ^h(1) BnNH_2 , DMF, 85 °C; (2) ArI, $\text{Pd}(\text{OAc})_2$, SPhos, K_3PO_4 , THF/ H_2O , 60 °C; ⁱTTMSS, DME, 85 °C; ^j NaOH , 30% H_2O_2 , THF, 0 °C to rt; ^k PhCOONa , DMF, 85 °C; ^l BnSH , Et_3N , DMF, 85 °C; ^m POCl_3 , MeCN, 110 °C. For more details, see the ESI.†

also performed using α -cyclopropylstyrene, which is considered to participate in radical rearrangement,^{36,37} as a probe (Scheme 5B). A ring-open difunctionalized product **77** was obtained in a 78% yield along with a *cis-trans* isomerization ratio of 5 : 1, and a trace amount of **23** was observed. Both results imply that a single-electron transfer pathway drove the generation of the difluoroalkyl radical, and the radical addition had priority over $\text{Pd}(\text{I})\text{--X}$ oxidative addition. To confirm the guiding role of B(MIDA), two comparative experiments in which vinyl Bpin and styrene were used to displace B(MIDA) as starting materials were conducted (Scheme 5C), and no target products were formed, which offered some evidence for capturing $\text{Pd}(\text{I})\text{--X}$ species by B(MIDA). As illustrated in Scheme 5D, no reaction occurred in the absence of the palladium catalyst, suggesting that the palladium catalyst was the key factor for fluoroalkyl-radical initiation. We chose another path involving a nickel





Scheme 5 Mechanistic studies.

catalyst and a bpy-ligand to observe whether the reaction would proceed given that nickel could also generate difluoroalkyl free radicals.³⁸ However, nearly no product was obtained, which was in sharp contrast to the model reaction. Besides, it was also unable to carry out the standard reaction thermally initiated by AIBN. Therefore, we added TEMPO trying to capture TEMPO- CF_2COOEt . Unfortunately, neither **76** nor **1** was detected by MS or ^{19}F NMR, which means that Ni(II) and AIBN are not a suitable initiator to induce the difluoroalkyl radical in our reaction system. Finally, deficiency of the base led to a remarkable decrease in the yield, which was <5%, as detected *via* ^{19}F NMR, further substantiating the idea that the alkali cation might be critical in inducing C-X formation.

Since we observed the unclear role of bases in our reaction system, to provide more insight into the role of the BMIDA group and observed selectivity, density functional theory (DFT) calculations were carried out with the Gaussian 16 package.³⁹ As shown in Fig. 1, the reactant **S-1** was selected as the zero-point of the potential energy surface ($0.0 \text{ kcal mol}^{-1}$). The direct generation of free radical **INT1** from **S-1** without the catalyst Pd-BINAP (**C1**) required a very high free energy barrier of $51.9 \text{ kcal mol}^{-1}$ (Fig. S1†), indicating that the Pd catalyst was essential to initiate the radical process and then form **INT1** and **C2**. As a reversible regio-selectivity was observed in compound **56**, two addition pathways were compared in both our model reaction and the formation of **56** (for **56**, see ESI Fig. S4†). In the model reaction, **INT1** underwent a radical-addition process with **B-1** to produce the key intermediate **P1-INT2** *via* transition state **P1-TS1** in the main reaction (pathway1) with a free energy barrier of

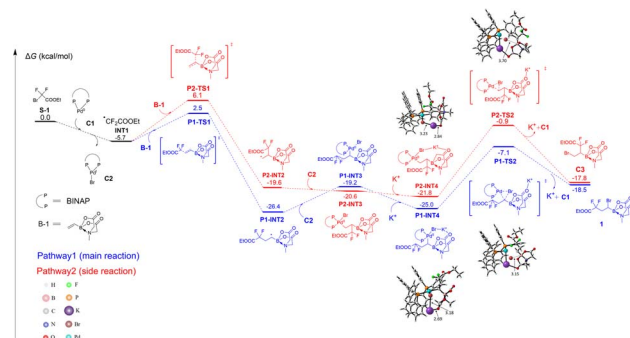


Fig. 1 Free-energy profile for the formation of **1** and **C3**, calculated at the M06-D3/6-311++G(d,p) SDD//B3LYP-D3(BJ)/6-31G(d) SDD level of theory. The SDD basis set was used for Pd. Free energies are given in kcal mol^{-1} .

$8.2 \text{ kcal mol}^{-1}$, which is more favorable than the side reaction (pathway2) *via* **P2-TS1** ($11.8 \text{ kcal mol}^{-1}$). **P1-INT2** or **P2-INT2** further reacted with **C2** to form the $\text{C(sp}^3\text{)-Pd(II)-X}$ system **P1-INT3** or **P2-INT3**, respectively, which was then stabilized by alkali metal cations (*e.g.* K^+) *via* its potential coulombic interaction with Br and carbonyl-O of BMIDA (**P1-INT4** and **P2-INT4**). Subsequently, Br was transferred to the $\alpha\text{-C}$ of the boron atom through direct RE to form the final product **1** *via* the transition state **P1-TS2** with a free energy barrier of $17.9 \text{ kcal mol}^{-1}$, which was lower than that *via* **P2-TS2** ($20.9 \text{ kcal mol}^{-1}$). Notably, it was found that the free energy barrier of the transition state **P1-TS_{NO}** without alkali metal cations (*e.g.* K^+) was $33.3 \text{ kcal mol}^{-1}$, indicating the critical role of the BMIDA-chelated alkali metal ion which enabled the sp^3 -reductive-elimination to proceed successfully (Fig. S2†). In addition, a weak attraction between B and Br was recognized by IGM^{40,41} analysis using Multiwfn,⁴² which could further stabilize the alkali metal ion complex and might be helpful for heterolytic Pd-X bond dissociation (Fig. S3†). Based on the DFT calculations, it could be concluded that **C1**, **BMIDA** and alkali metal carbonates (*e.g.* K_2CO_3) were important to the reaction of **S-1** and **B-1** to form the product **1**; moreover, generally observed thermodynamic and dynamic stability made pathway1 feasible while regio-reversible pathway2 was not.

However, it should be mentioned that XAT (halogen atom transfer) could also be another possible pathway which occurred in our reaction system.^{35g} Once the fluoroalkyl-radical is initiated by Pd(0), halogens of the other difluoroalkyl halides might be abstracted and therefore form the product as well as create a new difluoroalkyl radical *via* the chain reaction mechanism. The Pd(I) species could also provide the halogens for the fluoroalkyl-radical and be reduced to Pd(0) at the same time. Research trying to find the correct mechanism is still ongoing.

Conclusions

In summary, a high-efficiency and facile synthesis of fluorinated α -halo boronates was established in this study. The anticipated functional groups of B(MIDA) and the alkali cation aided the direct reductive elimination of the $\text{C(sp}^3\text{)-Pd(II)-X}$ system,



which was fully characterized by DFT calculations. A series of useful trifunctionalized (F, X, B) building blocks were furnished through the designed plan. This catalytic strategy provides extensive access to esters, amides, drugs, and even natural products modified with fluorinated α -halo boronates, and demonstrates a high level of functional group tolerance, which is unusual for these types of products. Additionally, the palladium-catalyzed process overcomes the challenges associated with substituted olefin boronates, thereby improving the possibilities for diverse functionalization. Follow-up decoration of the products further expands the variety and verifies the practicality of this method. This unique protocol has immense potential for application in the drug industry and chemical biology and will pave a new path for the synthesis of organo-boron compounds.

Data availability

All experimental, DFT calculation and characterization data, as well as NMR spectra are available in the ESI.† Crystallographic data for compound **23** have been deposited in the Cambridge Crystallographic Data Centre under accession number CCDC 2236620.

Author contributions

W. Z., C. L. and H. L. conceived this project. H. W., R. L., W. Z., C. L., and H. L. designed the experiments. H. W. performed the experiments. J. P. and R. Z. prepared some starting materials. R. L., Z. H. and Z. X. performed DFT calculations. H. W., R. L., W. Z., C. L., and H. L. analyzed and interpreted the results. H. W., R. L., W. Z., C. L., and H. L. wrote and revised this manuscript.

Conflicts of interest

There are no conflicts to declare.

Acknowledgements

We are grateful to the National Key R&D Program of China (No. 2023YFF1205104 and 2022YFA1302900), the National Natural Science Foundation of China (No. 82273766 and 82130105), and the Youth Innovation Promotion Association CAS (2020282). We thank LetPub (<https://www.letpub.com/>) for its linguistic assistance during the preparation of this manuscript.

Notes and references

- O. Andler and U. Kazmaier, *Org. Lett.*, 2021, **23**, 8439.
- O. Andler and U. Kazmaier, *Org. Biomol. Chem.*, 2021, **19**, 4866.
- J. Gorges and U. Kazmaier, *Org. Lett.*, 2018, **20**, 2033.
- Y. Lou, J. Qiu, K. Yang, F. Zhang, C. Wang and Q. Song, *Org. Lett.*, 2021, **23**, 4564.
- D. S. Matteson, H.-W. Man and O. C. Ho, *J. Am. Chem. Soc.*, 1996, **118**, 4560.
- S. Z. Sun, M. Borjesson, R. Martin-Montero and R. Martin, *J. Am. Chem. Soc.*, 2018, **140**, 12765.
- S. Z. Sun and R. Martin, *Angew. Chem., Int. Ed.*, 2018, **57**, 3622.
- J. Schmidt, J. Choi, A. T. Liu, M. Slusarczyk and G. C. Fu, *Science*, 2016, **354**, 1265.
- (a) R. Smoum, A. Rubinstein, V. M. Dembitsky and M. Srebnik, *Chem. Rev.*, 2012, **112**, 4156; (b) S. Touchet, F. Carreaux, B. Carboni, A. Bouillon and J. L. Boucher, *Chem. Soc. Rev.*, 2011, **40**, 3895; (c) D. B. Diaz and A. K. Yudin, *Nat. Chem.*, 2017, **9**, 731; (d) V. M. Dembitsky and M. Srebnik, *Tetrahedron*, 2003, **59**, 579; (e) E. S. Priestley and C. P. Decicco, *Org. Lett.*, 2000, **2**, 3095.
- (a) D. S. Matteson, *J. Org. Chem.*, 2013, **78**, 10009; (b) D. S. Matteson, *Chem. Rev.*, 1989, **89**, 1535; (c) D. S. Matteson and D. Majumdar, *J. Am. Chem. Soc.*, 1980, **102**, 7588; (d) D. S. Matteson and D. Majumdar, *Organometallics*, 1983, **2**, 1529.
- (a) S. Elgindy, G. Patel, V. V. Kakkar, G. Claeson, D. Green, E. Skordalakes, J. A. Baban and J. Deadman, *Tetrahedron Lett.*, 1994, **35**, 2435; (b) S. Elgindy, G. Claeson, V. V. Kakkar, D. Green, G. Patel, C. A. Goodwin, J. A. Baban, M. F. Scully and J. Deadman, *Tetrahedron*, 1994, **50**, 3803.
- (a) B. Zheng and M. Srebnik, *Tetrahedron Lett.*, 1993, **34**, 4133; (b) B. Zheng and M. Srebnik, *Tetrahedron Lett.*, 1994, **35**, 1145.
- (a) D. J. Pasto, J. Chow and S. K. Arora, *Tetrahedron*, 1969, **25**, 1557; (b) H. C. Brown, N. R. De Lue, Y. Yamamoto and K. Maruyama, *J. Org. Chem.*, 1977, **42**, 3252; (c) D. S. Matteson and D. Fernando, *J. Organomet. Chem.*, 2003, **680**, 100; (d) H. C. Brown and Y. Yamamoto, *J. Chem. Soc. D*, 1971, 1535.
- L. Yang, D. H. Tan, W. X. Fan, X. G. Liu, J. Q. Wu, Z. S. Huang, Q. Li and H. Wang, *Angew. Chem., Int. Ed.*, 2021, **60**, 3454.
- D. Wang, J. Zhou, Z. Hu and T. Xu, *J. Am. Chem. Soc.*, 2022, **144**, 22870.
- (a) Y. Zhou, J. Wang, Z. Gu, S. Wang, W. Zhu, J. L. Aceña, V. A. Soloshonok, K. Izawa and H. Liu, *Chem. Rev.*, 2016, **116**, 422; (b) J. Wang, M. Sanchez-Rosello, J. L. Acena, C. del Pozo, A. E. Sorochinsky, S. Fustero, V. A. Soloshonok and H. Liu, *Chem. Rev.*, 2014, **114**, 2432.
- Y. Ogawa, E. Tokunaga, O. Kobayashi, K. Hirai and N. Shibata, *iScience*, 2020, **23**, 101467.
- X. Chen, K. Fan, Y. Liu, Y. Li, X. Liu, W. Feng and X. Wang, *Adv. Mater.*, 2022, **34**, e2101665.
- (a) K. Marcin, D. Marek, D. Krzysztow, K. Tomasz, S. Janusz and W. Krzysztow, *Tetrahedron Lett.*, 2017, **58**, 2162; (b) M. Ueda, Y. Kato, N. Taniguchi and T. Morisaki, *Org. Lett.*, 2020, **22**, 6234; (c) T. Fang, J. Qiu, K. Yang and Q. Song, *Org. Chem. Front.*, 2021, **8**, 1991.
- (a) J. Li and M. D. Burke, *J. Am. Chem. Soc.*, 2011, **133**, 13774; (b) D. M. Knapp, E. P. Gillis and M. D. Burke, *J. Am. Chem. Soc.*, 2009, **131**, 6961; (c) E. M. Woerly, A. H. Cherney, E. K. Davis and M. D. Burke, *J. Am. Chem. Soc.*, 2010, **132**, 6941; (d) G. R. Dick, E. M. Woerly and M. D. Burke, *Angew. Chem., Int. Ed.*, 2012, **51**, 2667; (e) E. M. Woerly, J. Roy and



- M. D. Burke, *Nat. Chem.*, 2014, **6**, 484; (f) J. Li, S. G. Ballmer, E. P. Gillis, S. Fujii, M. J. Schmidt, A. M. E. Palazzolo, J. W. Lehmann, G. F. Morehouse and M. D. Burke, *Science*, 2015, **347**, 1221; (g) A. M. Kelly, P.-J. Chen, J. Klubnick, D. J. Blair and M. D. Burke, *Org. Lett.*, 2020, **22**, 9408; (h) D. J. Blair, S. Chitti, M. Trobe, D. M. Kostyra, H. M. S. Haley, R. L. Hansen, S. G. Ballmer, T. J. Woods, W. Wang, V. Mubayi, M. J. Schmidt, R. W. Pipal, G. F. Morehouse, A. M. E. Palazzolo Ray, D. L. Gray, A. L. Gill and M. D. Burke, *Nature*, 2022, **604**, 92.
- 21 (a) S. Adachi, A. B. Cognetta, M. J. Niphakis, Z. He, A. Zajdlík, J. D. St Denis, C. C. Scully, B. F. Cravatt and A. K. Yudin, *Chem. Commun.*, 2015, **51**, 3608; (b) A. Holownia, C. H. Tien, D. B. Diaz, R. T. Larson and A. K. Yudin, *Angew. Chem., Int. Ed.*, 2019, **58**, 15148; (c) S. J. Kaldas, C. H. Tien, G. D. P. Gomes, S. Meyer, M. Sirvinskas, H. Foy, T. Dudding and A. K. Yudin, *Org. Lett.*, 2021, **23**, 324.
- 22 (a) M. L. Lepage, S. Lai, N. Peressin, R. Hadjerci, B. O. Patrick and D. M. Perrin, *Angew. Chem., Int. Ed.*, 2017, **56**, 15257; (b) Y. M. Ivon, I. V. Mazurenko, Y. O. Kuchkovska, Z. V. Voitenko and O. O. Grygorenko, *Angew. Chem., Int. Ed.*, 2020, **59**, 18016.
- 23 (a) W. X. Lv, Y. F. Zeng, Q. Li, Y. Chen, D. H. Tan, L. Yang and H. Wang, *Angew. Chem., Int. Ed.*, 2016, **55**, 10069; (b) Y. F. Zeng, W. W. Ji, W. X. Lv, Y. Chen, D. H. Tan, Q. Li and H. Wang, *Angew. Chem., Int. Ed.*, 2017, **56**, 14707; (c) W. X. Lv, Q. Li, J. L. Li, Z. Li, E. Lin, D. H. Tan, Y. H. Cai, W. X. Fan and H. Wang, *Angew. Chem., Int. Ed.*, 2018, **57**, 16544; (d) D. H. Tan, Y. H. Cai, Y. F. Zeng, W. X. Lv, L. Yang, Q. Li and H. Wang, *Angew. Chem., Int. Ed.*, 2019, **58**, 13784.
- 24 G.-W. Yang, Y.-Y. Zhang, R. Xie and G.-P. Wu, *J. Am. Chem. Soc.*, 2020, **142**, 12245.
- 25 G.-W. Yang, C.-K. Xu, R. Xie, Y.-Y. Zhang, X.-F. Zhu and G.-P. Wu, *J. Am. Chem. Soc.*, 2021, **143**, 3455.
- 26 Y.-Y. Zhang, G.-W. Yang, R. Xie, X.-F. Zhu and G.-P. Wu, *J. Am. Chem. Soc.*, 2022, **144**, 19896.
- 27 (a) D. T. Rosevear and F. G. A. Stone, *J. Chem. Soc. A*, 1968, 164; (b) H. D. Empsall, M. Green and F. G. A. Stone, *J. Chem. Soc., Dalton Trans.*, 1972, 96; (c) Q.-Y. Chen, Z.-Y. Yang, C.-X. Zhao and Z.-M. Qiu, *J. Chem. Soc., Perkin Trans. 1*, 1988, 563.
- 28 Z. Feng, Q. Q. Min, H. Y. Zhao, J. W. Gu and X. Zhang, *Angew. Chem., Int. Ed.*, 2015, **54**, 1270.
- 29 B. Quiclet-Sire and S. Z. Zard, *J. Am. Chem. Soc.*, 2015, **137**, 6762.
- 30 N. Kumar, R. R. Reddy, N. Eghbarieh and A. Masarwa, *Chem. Commun.*, 2019, **56**, 13.
- 31 X. Chen, J. Zhao, M. Dong, N. Yang, J. Wang, Y. Zhang, K. Liu and X. Tong, *J. Am. Chem. Soc.*, 2021, **143**, 1924.
- 32 Y. Lan, P. Liu, S. G. Newman, M. Lautens and K. N. Houk, *Chem. Sci.*, 2012, **3**, 1987.
- 33 J. Z. Essman and E. N. Jacobsen, *J. Am. Chem. Soc.*, 2024, **146**, 7165.
- 34 N. A. Meanwell, *J. Med. Chem.*, 2018, **61**, 5822.
- 35 (a) C. Xu, R. Cheng, Y. C. Luo, M. K. Wang and X. Zhang, *Angew. Chem., Int. Ed.*, 2020, **59**, 18741; (b) L. An, Y. L. Xiao, S. Zhang and X. Zhang, *Angew. Chem., Int. Ed.*, 2018, **57**, 6921; (c) H. Y. Zhao, Z. Feng, Z. Luo and X. Zhang, *Angew. Chem., Int. Ed.*, 2016, **55**, 10401; (d) L. An, F. F. Tong, S. Zhang and X. Zhang, *J. Am. Chem. Soc.*, 2020, **142**, 11884; (e) X.-P. Fu, X.-S. Xue, X.-Y. Zhang, Y.-L. Xiao, S. Zhang, Y.-L. Guo, X. Leng, K. N. Houk and X. Zhang, *Nat. Chem.*, 2019, **11**, 948; (f) C. Xu, Z.-F. Yang, L. An and X. Zhang, *ACS Catal.*, 2019, **9**, 8224; (g) W.-H. Guo, H.-Y. Zhao, Z. J. Luo, S. Zhang and X. Zhang, *ACS Catal.*, 2019, **9**, 38.
- 36 J. E. Baldwin, *Chem. Rev.*, 2003, **103**, 1197.
- 37 E. Shirakawa, X. Zhang and T. Hayashi, *Angew. Chem., Int. Ed.*, 2011, **50**, 4671.
- 38 J. W. Gu, Q. Q. Min, L. C. Yu and X. Zhang, *Angew. Chem., Int. Ed.*, 2016, **55**, 12270.
- 39 M. Frisch, G. Trucks, H. B. Schlegel, G. Scuseria, M. Robb, J. Cheeseman, G. Scalmani, V. Barone, G. Petersson and H. Nakatsuji, *Gaussian 16*, Gaussian, Inc., Wallingford CT, 2016.
- 40 C. Lefebvre, G. Rubez, H. Khartabil, J.-C. Boisson, J. Contreras-García and E. Hénon, *Phys. Chem. Chem. Phys.*, 2017, **19**, 17928.
- 41 T. Lu and Q. Chen, *J. Comput. Chem.*, 2022, **43**, 539.
- 42 T. Lu and F. Chen, *J. Comput. Chem.*, 2012, **33**, 580.

